FEBS Letters 547 (2003) 20–26 FEBS 27413

Preferential closed channel blockade of HERG potassium currents by chemically synthesised BeKm-1 scorpion toxin

James T. Milnes[a], Christopher E. Dempsey[b], John M. Ridley[a], Olivia Crociani[c], Annarosa Arcangeli[c], Jules C. Hancox[a], Harry J. Witchel[a,*]

[a] *Department of Physiology and Cardiovascular Research Laboratories, School of Medical Sciences, University of Bristol, University Walk, Bristol BS8 1TD, UK*
[b] *Department of Biochemistry, School of Medical Sciences, University of Bristol, University Walk, Bristol BS8 1TD, UK*
[c] *Department of Experimental Pathology and Oncology, University of Firenze, Viale G.B. Morgagni 50, 50134 Florence, Italy*

Received 1 April 2003; revised 29 May 2003; accepted 6 June 2003

First published online 17 June 2003

Edited by Maurice Montal

Abstract The scorpion toxin peptide BeKm-1 was synthesised by fluorenylmethoxycarbonyl solid phase chemistry and folded by air oxidation. The peptide's effects on heterologous human *ether-a-go-go*-related gene potassium current (I_{HERG}) in HEK293 cells were assessed using 'whole-cell' patch clamp. Blockade of I_{HERG} by BeKm-1 was concentration-dependent, temperature-dependent, and rapid in onset and reversibility. Blockade also exhibited inverse voltage dependence, inverse dependence on duration of depolarisation, and reverse use- and frequency-dependence. Blockade by BeKm-1 and recombinant ergtoxin, another scorpion toxin known to block HERG, differed in their recovery from HERG current inactivation elicited by strong depolarisation and in their ability to block HERG when the channels were already activated. We conclude that synthetic BeKm-1 toxin blocks HERG preferentially through a closed (resting) state channel blockade mechanism, although some open channel blockade also occurs.

Key words: BeKm-1; Ergtoxin; Human *ether-a-go-go*-related gene; I_{Kr}; Rapid delayed rectifier; Scorpion toxin; *Buthus eupeus*; *Centruroides noxius*

1. Introduction

An understanding of human *ether-a-go-go*-related gene (HERG) potassium (K^+) channel blockade by drugs is critical because of its link to acquired long QT syndrome [1,2]. In an effort to understand how HERG blockade relates to cardiotoxic risk, the mechanism of blockade has been elucidated for a growing number of HERG blocking agents, in terms of both molecular determinants and state dependence of blockade. Virtually all of the drugs for which relevant mechanistic information is available are open/inactivated channel blockers [3], and most are also thought to access the site of blockade from inside the cell (e.g. [4,5]). Presumably, these drugs (which are small molecules) can cross the plasma membrane in an uncharged state, and when the channel is open, these drugs can access their site of action inside the HERG channel vestibule from the cytoplasmic side of the channel [6]. Recent structural data on K^+ channels suggest that the selectivity filter at the extracellular side of such channels is too small to allow drugs to pass through to the channel vestibule, whereas the vestibule would be more accessible from the cytoplasmic side of the channel, although this access could occur only when the channel is open [7–9].

Compared to other HERG blockers (i.e. small molecules and drugs), the two known scorpion toxin peptides that potently block HERG are unusual in that they are thought to act from the extracellular side of the membrane. One such toxin, ergtoxin from *Centruroides noxius*, has been shown to have molecular determinants of blockade in the extracellular S5-pore linker region, also called the 'turret' [10,11]. Another such toxin, BeKm-1 from the scorpion *Buthus eupeus*, has been shown, at room temperature, to block M-like currents from NG108-15 mouse neuroblastoma×rat glioma cells and heterologous HERG currents in human embryonic kidney (HEK293) cells and in *Xenopus* oocytes [12–14].

Since the positively charged, 36 amino acid BeKm-1 peptide is unlikely to cross the plasma membrane easily, it probably does not access its site of action from inside the cell, and as such BeKm-1 may also differ in its state dependence of blockade from other HERG blockers. Relatively little is known about the channel 'state dependence' of the BeKm-1 peptide's action on HERG. Therefore, we have used fluorenylmethoxycarbonyl (Fmoc) chemistry and air oxidation to synthesise successfully an active BeKm-1 peptide, and we report this method here. In addition, we have addressed the deficit in information on BeKm-1's state dependence of blockade, particularly in its actions at 37°C, because HERG's conductance and kinetics (and those of its homologues) at 37°C differ dramatically from these properties at room temperature [15,16]. We present evidence for a primarily closed (resting) state-dependent blockade of HERG, demonstrated by an inverse voltage dependence, negative time dependence, and reverse use and frequency dependence (e.g. [17]).

*Corresponding author. Fax: (44)-117-928 8923.
E-mail address: harry.witchel@bristol.ac.uk (H.J. Witchel).

Abbreviations: ANOVA, analysis of variance; CI, 95% confidence intervals; DQF-COSY, double quantum filtered correlation spectroscopy; Fmoc, fluorenylmethoxycarbonyl; *h*, Hill coefficient; HEK, human embryonic kidney; HERG, human *ether-a-go-go*-related gene; HPLC, high performance liquid chromatography; IC_{50}, half-maximal inhibitory drug concentration; I_{HERG}, current mediated by the HERG channel; *k*, slope factor describing voltage-dependent activation; rBeKm-1, recombinant BeKm-1; S-to-S, start-to-start interval; $V_{0.5}$, half-maximal activation voltage

0014-5793/03/$22.00 © 2003 Published by Elsevier Science B.V. on behalf of the Federation of European Biochemical Societies.
doi:10.1016/S0014-5793(03)00662-8

2. Materials and methods

2.1. Cells and electrophysiology

The HEK293 cell line stably expressing HERG (generously donated by Professor Craig January, University of Wisconsin [15]), its maintenance, electrophysiological recording and conditions (including Tyrode superfusate and K^+-based pipette solution), as well as methods for capacitance and series resistance compensation, the experimental apparatus, data acquisition, digitisation and analysis (including formulae for fractional block, Hill fit, and Boltzmann fit) have been described in detail previously [18]. This cell line is commonly used in the assay of drug blocking effects on HERG (e.g. [19]), and its endogenous transient outward current on repolarisation to −40 mV (the voltage where tail currents are assayed in this study) is negligible [15,20]. On achieving whole-cell configuration, sufficient time was allowed to elapse to negate the effect of any time-dependent changes in half-maximal activation voltage ($V_{0.5}$) that can be observed with this cell line. All experiments were performed at 37°C with the exception of concentration–response experiments that were also conducted at room temperature.

2.2. Data analysis and presentation

Data are presented as mean ± S.E.M. with the exception of IC_{50}, which is shown as mean plus 95% confidence intervals (CI). Statistical comparisons were made using either a paired or unpaired two-tailed Student's *t*-test, a one-way analysis of variance (ANOVA) with a Bonferroni post-test using Prism 3 software (Graphpad) or two-way ANOVA using Intercooled Stata 7 (Stata, College Station, TX, USA). *P* values of less than 0.05 were taken as statistically significant.

2.3. Drugs

In house Fmoc-synthesised BeKm-1 (referred to as BeKm-1 throughout the remaining text) and commercially available recombinant BeKm-1 toxin (rBeKm-1, Alomone, Israel) and recombinant ergtoxin (Alomone) were dissolved in sterile 10 mM Tris–HCl, 1 mM EDTA, pH 7.6 to produce stock solutions of 25 μM. Stock solutions were aliquoted into glass vials and stored at −20°C until use. Stock solutions were added to normal Tyrode's solution to make up the concentrations referred to in Section 3. Solutions containing drug were made up fresh each experimental day and applied via a rapid solution delivery system [21].

2.4. Spectroscopy

Circular dichroism spectra were obtained at 20°C using a Jobin-Yvon CD6 spectropolarimeter, in H_2O at pH 4.5 at a concentration of 0.1 mg/ml in 0.2 cm path-length quartz cuvettes. Spectra are averages of five scans with peptide-free blanks subtracted. High resolution nuclear magnetic resonance (NMR) spectra (2 mM peptide concentration; pH 4.5) were obtained on the Jeol Alpha-500 NMR spectrometer of the Bristol Centre for Molecular Recognition. NMR acquisition and spectral assignment methods were similar to those described previously [22].

3. Results and discussion

3.1. Chemical synthesis, folding and characterisation of scorpion toxin peptide BeKm-1

The polypeptide was synthesised within the Protein and DNA facility of the Bristol Centre for Molecular Recognition using Fmoc chemistry. This is a new method for obtaining BeKm-1, as all previous work has used either bacterial over-expression [13,23] or direct purification from the crude scorpion venom [12]. The linear peptide was purified by high performance liquid chromatography (HPLC), using a linear gradient of acetonitrile in water containing 0.1% trifluoroacetic acid, using methods described previously [24,25]. The purified linear peptide was characterised by mass spectrometry, and was air-oxidised at room temperature in the dark by dissolving (at a concentration of 1 mg/ml) in 50 mM Tris–HCl, 1 mM EDTA (pH 9.0), which was thoroughly pre-aerated by shaking before dissolving the peptide [25]. The peptide was fully converted within 48 h to a single species that eluted from the HPLC column at a lower acetonitrile concentration than the non-oxidised peptide (i.e. more polar, which is consistent with the burial of hydrophobic side chains). The oxidised peptide was repurified by HPLC using the same conditions as for the reduced peptide (overall final yield from all purification and preparation steps was ∼10 mg per 100 mg of crude synthetic peptide).

Oxidation of BeKm-1 was accompanied by the adoption of secondary structure (particularly β-structure; see Fig. 1A), consistent with this class of disulphide-bonded toxins (e.g. maurotoxin [26]; HsTX1 [27]). The circular dichroism spectrum of the oxidised peptide is very similar to the spectrum recently reported for a recombinant version of BeKm-1 [23], with a minimum ellipticity near 217 nm, having a value of ∼−13 000 deg cm^2/dmol. Although the peptide did not run well on the MALDI mass spectrometer, oxidation of the reduced peptide resulted in a shift in apparent molecular mass from 4099 to 4094 mass units (expected molecular masses of 4098 and 4092 [13] for the reduced and oxidised peptides, respectively). Confirmation of the correct (native) disulphide bridge pattern, overall conformation and peptide purity was determined by assignment of the high resolution NMR spectrum of the oxidised peptide (at 500 MHz). Fig. 1B illustrates the CHα CHβ region of the double quantum filtered correlation spectroscopy (DQF-COSY) spectrum of synthetic, oxidised BeKm-1, in which correlation signals for every amino residue are resolved. A single set of signals is observed, indicating a single structural and conformational isomer. The chemical shifts of NH, CHα and CHβ protons are the same (within 0.1 ppm) as the values deposited (BioMagRes Bank; accession number 5184) for the toxin produced in *Escherichia coli* [23]. These results confirm that air oxidation of the synthetic BeKm-1 linear peptide, under the conditions described, results in the native disulphide bond arrangement and overall native fold, and yields a peptide that is equivalent to that produced by bacterial over-expression. This may provide a useful tool to allow large-scale production of BeKm-1 for comprehensive pharmacological characterisation and use.

3.2. BeKm-1 toxin potency of I_{HERG} blockade varies with pre-pulse duration and temperature

Fig. 2A highlights the rapidity and reversibility with which synthetic BeKm-1 block of HERG tail current (I_{HERG}) occurred. Fig. 2A shows representative current records in the absence, presence and following wash-out of 50 nM BeKm-1, whilst in Fig. 2B tail current amplitude for the same experiment is plotted as a function of pulse number. The potency of blockade observed under these conditions was substantially less than the BeKm-1 potency previously reported using mammalian cells at room temperature in response to a 400 ms depolarising pulse (IC_{50} = 3.3 nM [13]). Fig. 2C shows that the effect of BeKm-1 at steady state on I_{HERG} tails elicited following 2000 ms and 400 ms depolarising pulses was greater with the shorter duration test pulse. The leftward shift of the concentration–response relationships for I_{HERG} tail fractional block for the shorter depolarisation (IC_{50} and Hill coefficient (*h*) unpaired *t*-test, $P < 0.0001$ and $P = 0.79$, respectively) suggests that an attenuation of I_{HERG} block occurred with increasing time at +20 mV. Similar experiments were performed at room temperature (n = 4–11 cells at each concentration), resulting in lower IC_{50} values. For 2000 ms and 400 ms de-

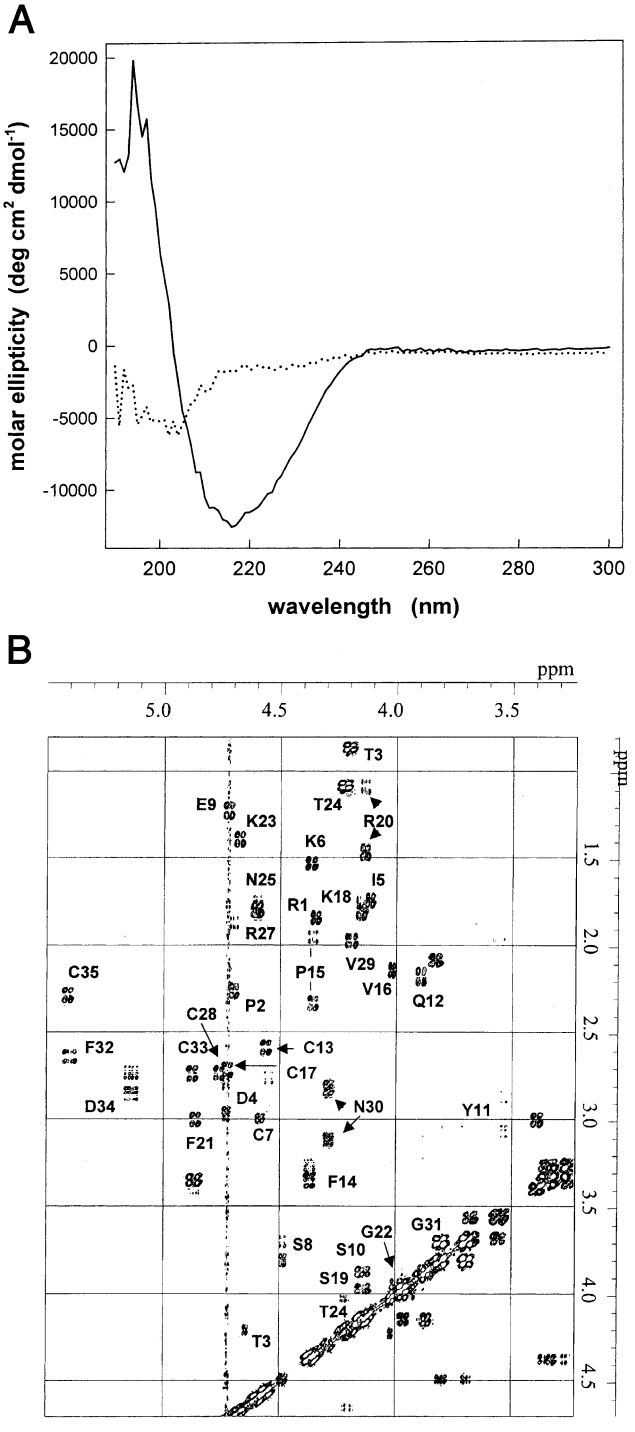

Fig. 1. Circular dichroism and NMR spectra of synthetic BeKm-1. A: Far UV circular dichroism spectra of purified synthetic BeKm-1 in H_2O at pH 4.5. The dotted and heavy lines correspond to spectra of the unoxidised (linear) peptide and the air-oxidised peptide, respectively. The units are molar ellipticity per residue. B: Region of the phase-sensitive DQF-COSY of air-oxidised BeKm-1 (in D_2O at pH* 4.5), with annotated cross-peaks correlating CHα and CHβ protons (and CHβ-CHγ protons of Thr).

polarisations, respectively, the IC_{50} values at room temperature were 9.7 nM (CI 7.2–13.0 nM) and 7.6 nM (CI 7.2–8.1 nM) and the Hill coefficients were 1.1 ± 0.1 and 1.1 ± 0.02 (the IC_{50} values are significantly different from one another, $P < 0.05$). At lower temperatures HERG gating kinetics will be slowed. Thus, temperature sensitivity of BeKm-1 blockade may be evidence for a gating process associated with depolarisation that relieves block.

To confirm the equivalence between the synthetic and recombinant BeKm-1, experiments identical to that reported in Fig. 2C were performed at 37°C using the commercially available rBeKm-1. rBeKm-1 inhibition of I_{HERG} tails (elicited at −40 mV) yielded IC_{50}s of 14.1 nM (CI 8.8–22.6 nM, *t*-test, $P > 0.7$ compared with BeKm-1) and 55.6 nM (CI 34.3–90.1 nM, *t*-test, $P > 0.53$ compared with BeKm-1) following an activating pulse to +20 mV for 400 or 2000 ms respectively ($n = 4$–11 cells at each of the six concentrations tested). Hill coefficients were also not statistically different when compared with the respective BeKm-1 concentration–response data (*t*-test, $P > 0.4$). rBeKm-1 also showed qualitatively similar temperature dependence of block (data not shown).

Additional time dependence experiments were performed at 37°C using the better characterised, but structurally dissimilar peptide HERG blocker, ergtoxin (10 nM). Similar to BeKm-1, fractional block was significantly decreased following a longer pre-pulse duration (2000 ms: 0.47 ± 0.02 and 400 ms: 0.65 ± 0.02, $n = 3$; paired *t*-test, $P < 0.002$).

3.3. Time-dependent blockade of I_{HERG} by BeKm-1 toxin

In order to study the time course of I_{HERG} blockade by BeKm-1, cells were held at −100 mV (at which all channels would be expected to be in the closed/resting state) and then subjected to a 'short depolarisation' (+40 mV for 10 ms) before I_{HERG} tails were observed at −40 mV. The elicited currents were compared in the absence and presence (first sweep) of BeKm-1 (25 nM); representative currents are shown in Fig. 2D. By observing the first tail current elicited in the presence of the toxin, this approach can detect (but not distinguish between) closed-state and extremely rapid (< 10 ms) open-state block – note that concentration-response measurements in Fig. 2C are based on measurements of steady-state blockade. Fractional block of I_{HERG} tail current during the protocol shown in Fig. 2D is 0.83 ± 0.03 ($n = 6$) (cf. 0.60 ± 0.02 following a 400 ms depolarising step). This is concordant with a closed-state blocking mechanism (or an extremely rapid open-state mechanism).

I_{HERG} blockade by open-channel blocking class III methanesulphonanilide agents during a sustained depolarisation shows a characteristic profile; it begins with virtually no blockade initially (i.e. for 1 s) and this progressively develops and increases over seconds during the maintained depolarisation [20,28]. In contrast, Fig. 2E shows that for BeKm-1 there is a time-dependent relief of fractional block during the first ~4 s of a sustained depolarising pulse (10 s) to 0 mV, from an initially high level to a lower steady-state level. Similar observations were made in three cells with rBeKm-1 (data not shown). A similar time-dependent relief of blockade by BeKm-1 was also found when using a stably transfected HERG-expressing cell line based on CHO cells that lack endogenous outward currents ($n = 4$ cells). Fig. 2F shows mean I_{HERG} fractional block data from Fig. 2E by BeKm-1 plotted at 100 ms intervals during the applied voltage pulse. A clear time-dependent relief of block is evident (ANOVA, $P < 0.0001$, $n = 6$ cells). Comparative 'long-pulse' experiments using 10 nM ergtoxin are also shown in Fig. 2F. Similar to BeKm-1, with a sustained depolarisation to 0 mV, a time-dependent relief of ergtoxin block was observed (ANOVA,

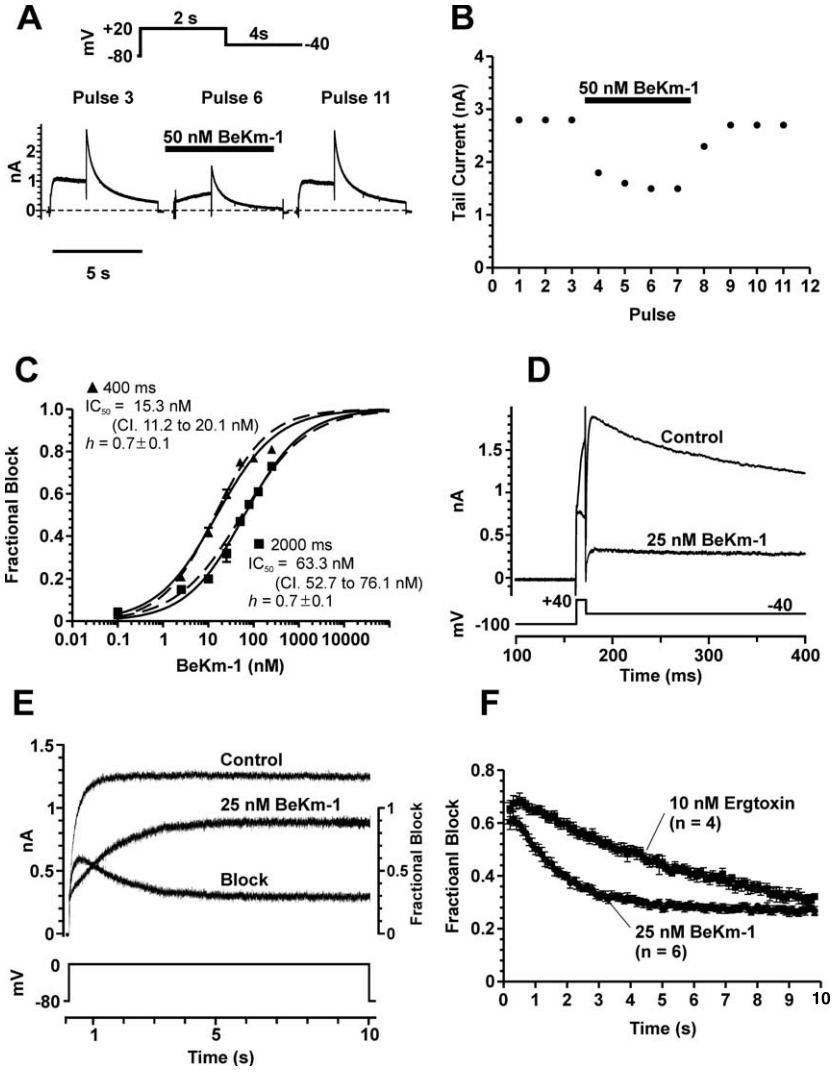

Fig. 2. Concentration- and time-dependent inhibition of HERG tail currents (I_{HERG}). A: Three concatenated current traces recorded from a typical cell at 37°C in the absence (left), presence (centre) and following washout (right) of 50 nM BeKm-1; voltage protocol (upper panel) was applied with a start-to-start (S-to-S) interval of 12 s. B: Summary of the tail current amplitude for the cell in A. Application of 50 nM BeKm-1 is indicated by the solid bar (typical of five cells). C: Mean fractional block data of I_{HERG} tails (plotted as a function of BeKm-1 concentration) resulting from command protocols at 37°C identical to that in A (2000 ms) and a similar protocol in which the depolarising step duration was shortened to 400 ms (S-to-S intervals of 12 and 10.4 s respectively to ensure similar durations spent at −80 mV). Data are fitted by a Hill equation (solid, intermittent lines). Symbols and solid lines, IC_{50} and h denote Fmoc-synthesised BeKm-1 data, intermittent line (no symbols shown) denotes concentration–response curves for rBeKm-1 using protocols and conditions identical to those used for BeKm-1. D: Representative tail current records (measured at −40 mV) following a 10 ms step to +40 mV in the absence and the first current trace following equilibration in 25 nM BeKm-1 (S-to-S interval = 12 s). During equilibration cells were held for 3 min at −100 mV to maintain channels in the closed state. E: Typical 'long pulse' current traces. The cell was repeatedly stepped to zero for 10 s from a holding potential of −80 mV (lower trace) to evoke stable steady-state currents (upper trace). Stimulation was then terminated and the cell was equilibrated in 25 nM BeKm-1 for >3 min whilst being held at −80 mV. The cell was then subjected to the same voltage command. Traces immediately prior to and the first step following equilibration in BeKm-1 are shown. Plotted on the same time axis is fractional block (right ordinate axis). F: Mean data (±S.E.M.) for the experiment in E ($n = 6$ cells). Time zero coincides with the voltage step from −80 mV to 0. For comparison identical experiments were performed using 10 nM ergtoxin. Mean data (±S.E.M.) for four cells are shown. Note that the initial rise in fractional block (which is not significant for either BeKm-1 or ergtoxin, ANOVA, $P > 0.05$) may correspond to the initial endogenous to heterologous current ratio diminishing over time.

$P < 0.0001$). However, the time course with which this occurred was substantially slower (single-exponential dissociation rate constant (K_{off}) at 0 mV 652.6 ± 29.0 ms^{-1} for ergtoxin compared with 134.8 ± 14.7 ms^{-1} for BeKm-1, t-test, $P < 0.00001$).

3.4. Voltage-dependent block of I_{HERG} by BeKm-1

The effect of test voltage (between −40 and +50 mV) on I_{HERG} tail current blockade by BeKm-1 was determined using the protocol illustrated in the upper panel of Fig. 3A. Mean data in panel A were fitted by a Boltzmann equation yielding a half-maximal activation ($V_{0.5}$; control −20.2 ± 1.0 mV compared with BeKm-1 −18.5 ± 2.8 mV, unpaired t-test, $P = 0.55$) and slope factor (k; control 6.2 ± 0.8 mV compared with BeKm-1 13.4 ± 1.8 mV, unpaired t-test, $P < 0.0005$). The likely reason the k values are doubled in BeKm-1 is that, whilst in control I_{HERG} tails reached a plateau between 0 and +40 mV, in the presence of BeKm-1 I_{HERG} tail magnitude

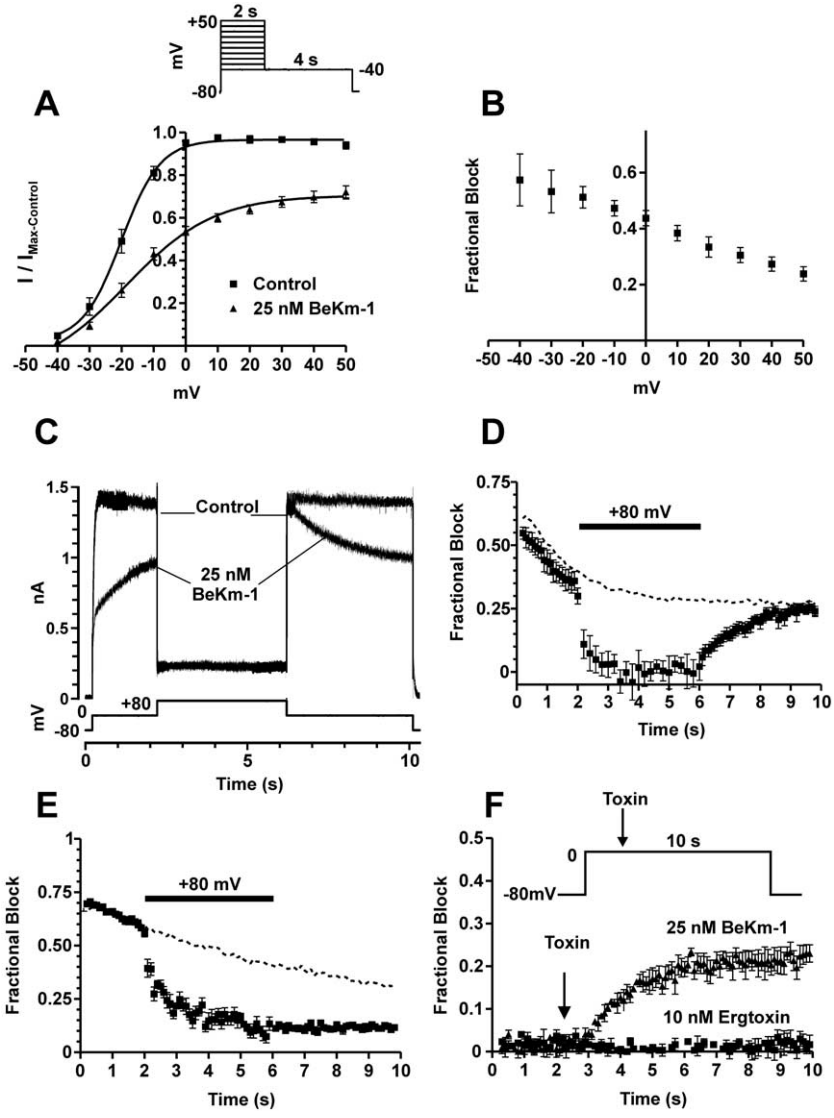

Fig. 3. Voltage-dependent block of I_{HERG} by BeKm-1. A: Mean I_{HERG} tail current data plotted as a function of test pulse potential (voltage protocol, upper panel) in the absence and presence of 25 nM BeKm-1. Current data for each cell are normalised to maximal tail current under control conditions ($n = 11$ cells). Data were fitted using a Boltzmann equation (solid lines). B: Mean fractional block of I_{HERG} tails plotted as a function of test voltage. C: Representative I_{HERG} traces (upper panel) in response to a modified long-pulse protocol with an additional 4 s step to +80 mV (lower panel). Experiments were performed as in Fig. 2E (i.e. measuring first sweep after equilibration in toxin). D: Mean (±S.E.M.) fractional block data obtained using this modified long-pulse protocol ($n = 6$ cells). E: Mean data from an identical experiment performed with 10 nM ergtoxin, in which re-development of block after the step from +80 mV to 0 mV never occurs. Intermittent lines in D and E indicate fractional block during the long-pulse protocol re-drawn from Fig. 2F. F: Effect of 'mid-pulse' application of either BeKm-1 or ergtoxin during a 10 s depolarising step from −80 mV to 0 (see inset). Arrows indicate the timing of the rapid solution switch from normal Tyrode's solution to normal Tyrode's containing the respective toxin. Mean fractional block ± S.E.M. ($n = 3$ cells in each group) is plotted as a function of time, with time zero corresponding to the depolarisation from −80 mV to 0.

tended to increase (relatively) over this potential range as block was reduced. Fig. 3B shows the tail current fractional block data plotted as a function of test potential. An inverse voltage dependence was observed (ANOVA, $P < 0.0001$). Inverse voltage dependence is concordant with closed state-dependent blockade. However this alone is not sufficient to prove closed-state blockade, as a HERG blockade attenuated by inactivation would also demonstrate inverse voltage dependence.

Diminished block with both increasing time and membrane potential may reflect an influence of channel inactivation upon BeKm-1's action. The potential role of inactivation was addressed further by depolarising HERG to a very positive potential (invoking profound inactivation) to determine whether or not I_{HERG} blockade was altered. Fig. 3C shows a modified long-pulse protocol, in which a 4 s depolarisation to +80 mV was applied from 0 [20,29,30]. Mean fractional block data from six cells tested as in Fig. 3C are plotted at 100 ms intervals in Fig. 3D. Depolarisation to +80 mV further reduced fractional block, approximating towards zero as the control and BeKm-1 currents converge. On repolarisation to 0, block can be seen to re-develop over time back to a level similar to that observed at the end of the protocol in Fig. 2F (intermittent line shown here has been redrawn from Fig. 2F), which is a 10s depolarising pulse to 0 mV lacking the interposed step to +80 mV. At +80 mV the preponderance of

HERG channels would be expected to be in the inactive state, and these data, therefore, support the idea that BeKm-1 does not primarily bind to the inactive channel state. Thus, the data are concordant with the potency of blockade for different channel states being closed > open ≫ inactivated. However, we are not able to exclude the possibility that the attenuation of blockade observed at +80 mV may involve a voltage-induced conformational change that is independent of inactivation. Similar observations were made in two cells with rBeKm-1 (data not shown).

Similar experiments using 10 nM ergtoxin are shown in Fig. 3E. As with BeKm-1, depolarisation to +80 mV during the long pulse resulted in decreased block in the presence of ergtoxin; this is consistent with the findings of Gurrola et al. [31]. However, unlike BeKm-1, ergtoxin block did not re-develop on repolarisation from +80 mV to 0 (ANOVA, $P > 0.75$). This characteristic of ergtoxin action has not been previously reported. The ability of BeKm-1 block of I_{HERG} to re-develop on repolarisation from +80 mV to 0, as inactivation is relieved and channels cycle back to the open state, suggests that BeKm-1 can also bind and block the open state channel, while ergtoxin does not. This may indicate that ergtoxin, in comparison with BeKm-1, has a mechanism of block more dependent on interacting with the closed state.

However, as depolarisation in the presence of ergtoxin does reveal the presence of some channel blockade (albeit one that diminishes with time), ergtoxin must – at least initially upon depolarisation – be able to block channels that have attained the open state. One possible explanation for this phenomenon is that ergtoxin can enter and remain in a blocking conformation with closed but not open HERG channels, although there is a time delay for ergtoxin's blockade to diminish when closed channels blocked by ergtoxin switch to the open conformation upon depolarisation. To test this, and thus determine whether ergtoxin and BeKm-1 differ in their ability to block open channels, experiments were performed in which each toxin was rapidly superfused onto the cells during the course of a depolarising pulse. Cell membrane potential was depolarised to 0 mV for 10 s, but the particular toxin was not added until 2 s after the beginning of the depolarisation (see Fig. 3F). Rapid superfusion of 25 nM BeKm-1 onto cells during depolarisation led to HERG blockade ($\sim 23 \pm 1\%$, which is of similar magnitude to that seen at the end of depolarisations in Fig. 2F), suggesting that BeKm-1 can block HERG channels in the open state. However, rapid superfusion of 10 nM ergtoxin onto cells during depolarisation did not lead to blockade ($\sim 2 \pm 1\%$), suggesting that ergtoxin cannot block HERG channels in the open state, except when the toxin has been previously allowed to interact with channels in the closed state. Considering the data presented concerning inverse time- and voltage-dependent block, these findings are concordant with ergtoxin's state dependence of blockade being closed ⋙ open ≥ inactivated. However, as for BeKm-1, it is feasible that alternative conformational changes independent of inactivation could contribute to the rapid diminution of ergtoxin block upon depolarisation to +80 mV.

3.5. Frequency- and use-dependence of BeKm-1 block of I_{HERG}

Collectively, the data in Figs. 2 and 3 suggest that BeKm-1 inhibits I_{HERG} by a mechanism that includes closed channel state blockade. Further to this, we investigated frequency- and use-dependence of block. A voltage protocol was applied with three different start-to-start (S-to-S) intervals (1.5, 3 and 24 s) and the degree of I_{HERG} tail block compared between them. Under control conditions, applying this protocol at these varying frequencies had no statistically significant effect on I_{HERG} tail amplitude ($n = 5$ cells, ANOVA, $P = 0.99$). For each cell, after a steady-state baseline was achieved in control

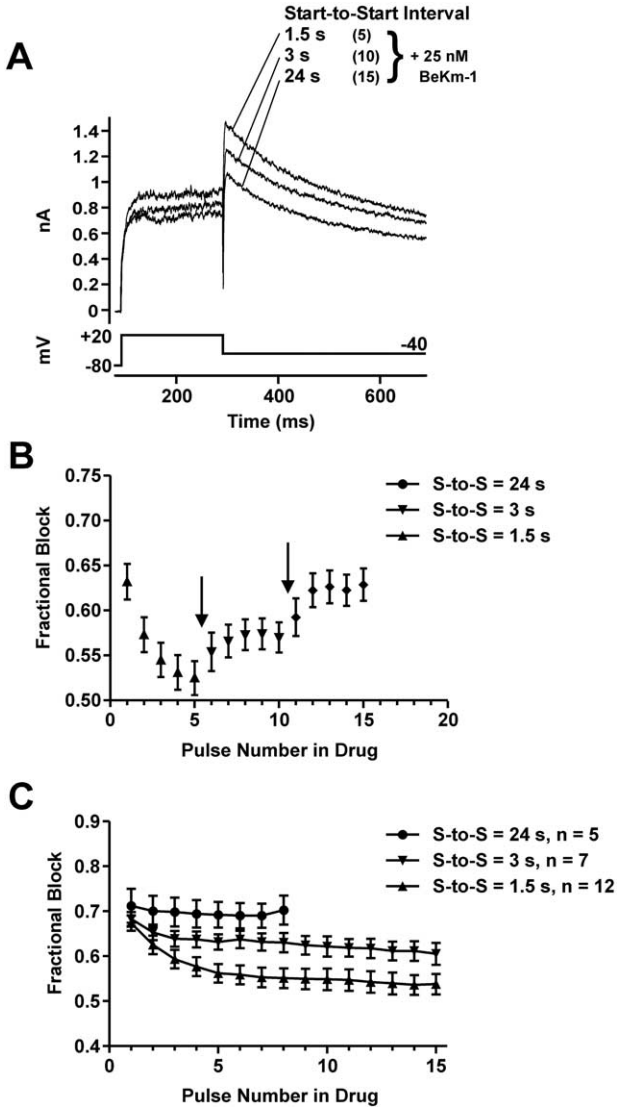

Fig. 4. Frequency- and use-dependent inhibition of I_{HERG} by BeKm-1. A: Representative current records from a cell in the presence of 25 nM BeKm-1, using a voltage protocol (lower panel) applied with three different S-to-S intervals. Numbers in parentheses correspond to pulse numbers in B; for this cell the peak tail current in control solution (not shown) was 3.5 nA. B: Mean fractional block of I_{HERG} tails. The protocol was applied with a S-to-S interval of 1.5 s to reach steady state in the absence of toxin. 25 nM BeKm-1 was then applied and the protocol repeated first with a S-to-S of 1.5 s (pulses 1–5) followed by 3 s (6–10) and finally 24 s (11–15). Arrows indicate changes in S-to-S interval. HERG channel block decreased with increased frequency of stimulation (ANOVA, $P < 0.001$). C: Use-dependent changes of BeKm-1 block of I_{HERG} tails. Cells were equilibrated in 25 nM BeKm-1 while held at −80 mV prior to being subjected to the same voltage command as in A applied at three different S-to-S intervals. Pulse 1 corresponds to the first pulse in BeKm-1. Fractional block was calculated relative to the corresponding control pulse in the absence of BeKm-1. Steady-state BeKm-1 block was smaller at higher stimulation rates (ANOVA, $P < 0.0001$).

solution, 25 nM BeKm-1 was applied and allowed to equilibrate at the −80 mV holding potential, and then stimulation was resumed at the highest frequency (pulse number 1, Fig. 4B). The S-to-S interval was then increased to 3 s and finally 24 s (indicated by arrows). Representative currents in the presence of toxin recorded in the same cell are shown in Fig. 4A, corresponding to pulses numbered 5, 10 and 15 of mean data in Fig. 4B. For the final time point at each frequency, HERG channel fractional block was significantly greater at slower stimulation frequencies (ANOVA with a Bonferroni post-test, $P < 0.001$). Use-dependence of BeKm-1 block was investigated using a voltage protocol identical to that shown in Fig. 4A applied at S-to-S intervals of 1.5, 3 and 24 s. Cells were paced at the respective frequency in the absence of BeKm-1, then allowed to equilibrate in 25 nM BeKm-1. Cells were then paced again at the same rate in the presence of BeKm-1 to study use-dependent changes of block. Fractional block was calculated relative to the corresponding pulse in control (Fig. 4C). Two-way ANOVA showed main effects for both frequency and pulse number ($P < 0.0001$ for each), replicating the frequency dependence effects in Fig. 4B; analysis of data from each frequency showed significant use-dependent effects for 1.5 s S-to-S (ANOVA, $P = 0.0004$), but not for 3 s ($P = 0.52$) or 24 s ($P = 0.99$). Overall, the inverse frequency- and reverse use-dependent data are concordant with the notion that BeKm-1 employs a preferential closed state mechanism in blocking HERG.

3.6. Conclusions

We have demonstrated a new method for the synthesis of functional BeKm-1. Under similar experimental conditions, synthesised BeKm-1 blocked I_{HERG} with identical potency to that of the commercially available rBeKm-1. BeKm-1 blockade of HERG varies inversely with temperature, time, voltage, use and frequency, and this has not been shown before for this or any other HERG blocking compound. BeKm-1, therefore, provides a striking example of an agent for which the degree of HERG blockade varies markedly depending upon the electrophysiological protocols (e.g. S-to-S interval) and conditions (e.g. temperature) used. The data suggest that the blockade is preferentially closed channel state-dependent, with a component of open, but not inactive, state-dependent blockade, and this is different from the mechanism of blockade by ergtoxin. This adds further weight to the argument that some blockers of HERG may act by a mechanism (and possibly at a site) distinct from the open state-dependent mechanism occurring at the high affinity site described within the vestibule [6], and future work will focus on whether such a site might play a role in HERG blockade by some drugs (as opposed to peptide toxins).

Acknowledgements: This work was supported by project grants from the British Heart Foundation to H.J.W. and J.C.H. (PG/2001104 and PG/2000123) and by a Wellcome Trust fellowship to J.C.H. The authors are grateful to Lesley Arberry, Terri Harding for technical assistance, Dr Graham Bloomberg for excellent synthesis of the linear BeKm-1 peptide, and David Robert Jones for the initial insight into toxins.

References

[1] Sanguinetti, M.C. and Keating, M.T. (1997) News Physiol. Sci. 12, 152–157.
[2] Tseng, G.N. (2001) J. Mol. Cell. Cardiol. 33, 835–849.
[3] Chen, J., Seebohm, G. and Sanguinetti, M.C. (2002) Proc. Natl. Acad. Sci. USA 99, 12461–12466.
[4] Mergenthaler, J., Haverkamp, W., Huttenhofer, A., Skryabin, B.V., Musshoff, U., Borggrefe, M., Speckmann, E.J., Breithardt, G. and Madeja, M. (2001) Naunyn Schmiedebergs Arch. Pharmacol. 363, 472–480.
[5] Zou, A., Curran, M.E., Keating, M.T. and Sanguinetti, M.C. (1997) Am. J. Physiol. 272, H1309–H1314.
[6] Mitcheson, J.S., Chen, J., Lin, M., Culberson, C. and Sanguinetti, M.C. (2000) Proc. Natl. Acad. Sci. USA 97, 12329–12333.
[7] Jiang, Y., Lee, A., Chen, J., Ruta, V., Cadene, M., Chait, B.T. and MacKinnon, R. (2003) Nature 423, 33–41.
[8] Jiang, Y., Lee, A., Chen, J., Cadene, M., Chait, B.T. and MacKinnon, R. (2002) Nature 417, 523–526.
[9] Doyle, D.A., Morais, C.J., Pfuetzner, R.A., Kuo, A., Gulbis, J.M., Cohen, S.L., Chait, B.T. and MacKinnon, R. (1998) Science 280, 69–77.
[10] Pardo-Lopez, L., Garcia-Valdes, J., Gurrola, G.B., Robertson, G.A. and Possani, L.D. (2002) FEBS Lett. 510, 45–49.
[11] Pardo-Lopez, L., Zhang, M., Liu, J., Jiang, M., Possani, L.D. and Tseng, G.N. (2002) J. Biol. Chem. 277, 16403–16411.
[12] Filippov, A.K., Kozlov, S.A., Pluzhnikov, K.A., Grishin, E.V. and Brown, D.A. (1996) FEBS Lett. 384, 277–280.
[13] Korolkova, Y.V., Kozlov, S.A., Lipkin, A.V., Pluzhnikov, K.A., Hadley, J.K., Filippov, A.K., Brown, D.A., Angelo, K., Strobaek, D., Jespersen, T., Olesen, S.P., Jensen, B.S. and Grishin, E.V. (2001) J. Biol. Chem. 276, 9868–9876.
[14] Zhang, M., Korolkova, Y.V., Liu, J., Jiang, M., Grishin, E.V. and Tseng, G.N. (2003) Biophys. J. 84, 3022.
[15] Zhou, Z., Gong, Q., Ye, B., Fan, Z., Makielski, J.C., Robertson, G.A. and January, C.T. (1998) Biophys. J. 74, 230–241.
[16] Wang, J., Della, P.K., Wang, H., Karczewski, J., Connolly, T.M., Koblan, K.S., Bennett, P.B. and Salata, J.J. (2003) Am. J. Physiol. 284, H256–H267.
[17] Campbell, D.L., Qu, Y., Rasmusson, R.L. and Strauss, H.C. (1993) J. Gen. Physiol. 101, 603–626.
[18] Milnes, J.T., Crociani, O., Arcangeli, A., Hancox, J.C. and Witchel, H.J. (2003) Br. J. Pharmacol. 139, 887–898.
[19] Caballero, R., Moreno, I., Gonzalez, T., Arias, C., Valenzuela, C., Delpon, E. and Tamargo, J. (2003) Circulation 107, 889–895.
[20] Snyders, D.J. and Chaudhary, A. (1996) Mol. Pharmacol. 49, 949–955.
[21] Levi, A.J., Hancox, J.C., Howarth, F.C., Croker, J. and Vinnicombe, J. (1996) Pflügers Arch. 432, 930–937.
[22] Halsall, A. and Dempsey, C.E. (1999) J. Mol. Biol. 293, 901–915.
[23] Korolkova, Y.V., Bocharov, E.V., Angelo, K., Maslennikov, I.V., Grinenko, O.V., Lipkin, A.V., Nosyreva, E.D., Pluzhnikov, K.A., Olesen, S.P., Arseniev, A.S. and Grishin, E.V. (2002) J. Biol. Chem. 277, 43104–43109.
[24] Takei, J., Remenyi, A., Clarke, A.R. and Dempsey, C.E. (1998) Biochemistry 37, 5699–5708.
[25] Dempsey, C.E., Sessions, R.B., Lamble, N.V. and Campbell, S.J. (2000) Biochemistry 39, 15944–15952.
[26] di Luccio, E., Matavel, A., Opi, S., Regaya, I., Sandoz, G., M'barek, S., Carlier, E., Esteve, E., Carrega, L., Fajloun, Z., Rochat, H., Loret, E., de Waard, M. and Sabatier, J.M. (2002) Biochem. J. 361, 409–416.
[27] Lebrun, B., Romi-Lebrun, R., Martin-Eauclaire, M.F., Yasuda, A., Ishiguro, M., Oyama, Y., Pongs, O. and Nakajima, T. (1997) Biochem. J. 328, 321–327.
[28] Spector, P.S., Curran, M.E., Keating, M.T. and Sanguinetti, M.C. (1996) Circ. Res. 78, 499–503.
[29] Kiehn, J., Lacerda, A.E., Wible, B. and Brown, A.M. (1996) Circulation 94, 2572–2579.
[30] Kiehn, J., Thomas, D., Karle, C.A., Schols, W. and Kubler, W. (1999) Naunyn Schmiedebergs Arch. Pharmacol. 359, 212–219.
[31] Gurrola, G.B., Rosati, B., Rocchetti, M., Pimienta, G., Zaza, A., Arcangeli, A., Olivotto, M., Possani, L.D. and Wanke, E. (1999) FASEB J. 13, 953–962.